International Journal of Nanoelectronics and Materials
IJNeaM
ISSN 1985-5761 | E-ISSN 2232-1535

# Hybrid PVDF/PET triboelectric nanogenerators with improved output for next-gen self-powered devices

Stephen Obeng Newton [a], Nur Syazana Rashidi [b] *, Nursyahirah Adnan [b], Nadhira Fathiah Kamarulzaman [b], Norzarina Ma'at [b], Nur Alia Shazmin Zakaria [b], Nurfadzylah Awang [b], Krishnan Subramaniam [b], and Rohit Nandakumar Shenoy [c]

[a]*Mechanical Engineering Studies, School of Engineering and Computing, MILA University, No 1, MIU Boulevard, Putra Nilai, 71800, Nilai, Negeri Sembilan, Malaysia*
[b]*Department of Mechanical Engineering, School of Engineering and Computing, MILA University, No 1, MIU Boulevard, Putra Nilai, 71800, Nilai, Negeri Sembilan, Malaysia*
[c]*Department of Mechanical & Industrial Engineering, Manipal Institute of Technology, Manipal Academy of Higher Education, Manipal, Karnataka, India*
** Corresponding author. Tel.: +606-7989200; e-mail: syazana.rashidi@mila.edu.my*

Received 19 January 2026, Revised 11 February 2026, Accepted 23 February 2026

**ABSTRACT**

With the rise in self-powered gadgets, triboelectric nanogenerators (TENGs) have emerged as a competent option for effective energy harvesting from mechanical motion. This research centers on the phenomenon of triboelectric charge generation at the interface of polyvinylidene fluoride (PVDF) and polyethylene terephthalate (PET) with respect to energy band theory. The study aims to improve the energy harvesting efficiency of TENGs through simulations and experimental work. Contact-separation TENG devices were constructed, and their performance was optimized using COMSOL software by varying parameters such as dielectric layer thickness, surface charge density, and distance. This work shows that TENG devices experience non-linear responses, which many traditional simulations fail to incorporate. Simulations alongside experimental results have shown that TENGs respond to applied force with voltage in a non-linear trend. Based on simulation results, the device has potential for substantial voltage generation; however, power density would benefit from improved geometric configuration and contact methods. This experimental validation supports simulation findings and highlights the PVDF/PET TENG's excellent energy-harvesting capability, even at the lower force levels. A major highlight of this study is that increasing dielectric spacing enhances output voltage and power density in dielectric–dielectric triboelectric nanogenerators. The application of this principle is thought to decrease the reliance on batteries, thereby addressing challenges related to recycling and disposal. This method could enable the advancement of more efficient and eco-friendly energy production and sensor technologies, suitable for applications in wearable electronics, healthcare, and industrial sectors.

**Keywords:** *PVDF, PET, Triboelectric nanogenerators, COMSOL*

## 1. INTRODUCTION

As technology continues to advance, the demand for energy to fuel our insatiable use of electronic devices has significantly increased. In the early days of electricity, devices had to be attached to a power source via cables to operate. The development of battery technology removed this constraint, allowing electronic devices to function wirelessly. This innovation not only improved the performance of electronic devices but also played a role in shifting away from reliance on fossil fuels for power generation [1].

In the contemporary era, utilizing natural resources represented an innovative method for producing electricity. This involves obtaining and converting the energy present in the environment, including sunlight, heat, vibrations, and other types of kinetic energy, into practical electricity. This process is commonly referred to energy scavenging or power harvesting and holds the capability to transform the methods of energy generation and utilization [2]. Most of the natural resources available for harvesting primarily exist in mechanical forms and can be harnessed through a variety of methods. For example, hydroelectric power generation founded on the utilization of potential energy retained in water stored at a specific elevation. Similarly, wind capture technologies such as wind turbines rely on the kinetic energy carried by wind to propel their turbines. These represent some of the remarkable strategies engineered to tap into energy resources from renewable and self-sustaining origins [3].

Out of all the available renewable energy sources in the present day, solar energy stands out as the most optimizable for domestic use. While small handheld devices can be equipped with solar panels for recharging using solar energy, such devices are rendered inactive during nighttime [4]. TENGs offer another avenue for energy harvesting for renewable energy. In TENGs, contact electrification with the device necessitates a minimum of two materials. Triboelectric materials produce polarized charges on all their surfaces while they are in operation, and these charges only occur momentarily. The contact of dissimilar materials introduces the triboelectric effect, which generates electric

charges. Chemical functionalization of the outermost surface layers, coupled with the micro- and nanotexturing of substrates, alongside elevated-design refinement of the devices, collectively amplify the transduction efficiency. Within the field of nanogenerator design, such interventions prove decisive, giving heightened electrostatic power output simultaneous with increased surface charge density during successive contact-separation phases. Additionally, the simultaneous activation of piezoelectric domains causes localized dipole realignments, which serve to supplement the triboelectric surface charge by successive accumulation, consequently increasing total energy harvesting competence [5].

This study evaluates enhancements in energy-harvesting capabilities achieved by TENGs using composite films of polyvinylidene fluoride (PVDF) and polyethylene terephthalate (PET). PET is widely established thermoplastic polymer, possesses a well-documented balance of mechanical rigidity and chemical inertness. These attributes permit PET to function successfully as a support and triboelectric layer within the mechanical structure of the TENGs [6]. The integration of PVDF into TENGs architecture has gained prominence owing to its combined piezoelectric and ferroelectric character. PVDF's increased dielectric constant, along with its significant piezoelectric response, makes PVDF an ideal dielectric medium, facilitating enhanced conversion efficiency and a high volumetric surface charge density at the nanoscale, thereby amplifying device power outputs effectively [7].

The limited energy production characteristic of PVDF/PET-based TENGs can be traced mechanically to an inadequate triboelectric charge density. The charge extraction mechanism is hindered by low electron mobility, leading to suboptimal transfer of triboelectric charge to the dielectric. The resultant accumulation on the polymeric surfaces is subcritical, thereby constraining the device's ultimate power output. When seen in conjunction with PET's dielectric constant of around 3.7, low-generation kinetics cause rapid charge decay, further lowering volumetric charge density. PET's intrinsic low work function, coupled with a comparably high surface energy, precludes stable charge confinement, necessitating investment of kinetic energy in overcoming energetic barriers that hinder accumulation. Collectively, the thermodynamic obstacles produce an inadequate triboelectric charge density, resulting in limited electrical energy generation [8, 9].

Additionally, the interfacial engineering of the heterostructure reveals intrinsic mismatches in charge density between PVDF's high polarity and PET's comparably low affinity. Composite interlayers thus suffer from adhesion micromorphologies, resulting in delamination precursors and giving rise to a multi-modal reduction in effective tribocharge density [9].

The high-explicit section surface topography of the PET polymer reveals a specific level of surface scattering and fault density, thereby further aggravating bulk polymer condition yield. Together, the interface charge affinities, delamination kinetics, and the control of defect-free polymeric films produce a resultant barrier to energy production and the large-scale employability of the corresponding design [8].

In this study, the charge generation mechanism of a hybrid PVDF/PET TENGs was explored using energy band theory, supported by both simulation and experimental data. The effects of TENG thickness, interlayer spacing, and applied force were studied to improve device output. The findings from this work are expected to assist in developing more advanced designs for the next generation of systems that are highly efficient and performance-driven, aiding the progress of self-powered systems.

## 2. METHODOLOGY

### 2.1. Simulation

Simulations were conducted in accordance with the guidelines captured in Table 1. The first stage involves simulating a metallic and dielectric system undergoing contact separation, then proceeding to simulate interactions between dielectric materials, which is depicted in Figure 1. Through these simulations, the process responsible for generating triboelectric charge, specifically the energy band, can be clarified.

Accordingly, a finite-element simulation model was implemented in COMSOL Multiphysics to improve both the energy-harvesting processes and the embedded sensing capabilities of patterned PVDF/PET triboelectric nanogenerator devices. The computational framework extends the analytical foundations originally articulated by Vasandani *et al.* (2016). The study examined the triboelectric phenomenon in a layered architecture utilizing polyethylene terephthalate and polyimide substrates, augmented by the nanometer-thick deposition of gold (Au) electrodes upon the respective dielectric matrices [10]. In contrast, this study used PVDF and PET as dielectric materials for nanogenerator devices. Identical parameter sets were subsequently implemented within the computational model.

The model includes detailed geometric, material, and electrical properties for the PVDF/PET stack, resulting in a complete, high-fidelity digital twin of the target device. Each assembly layer, electrical contacts, dielectric, and metal electrodes, has been incorporated as discrete entities, employing calibrated mechanical and electrical properties to capture both quasi-static and dynamic modes of operation. Particular emphasis is placed on the contact-separation mechanism, which, as the primary dynamic process, is responsible for the development of charge through surface field reorganization. The behavioral micro-

**Table 1.** Data collection table [10]

| Parameter | Value/Description |
|---|---|
| Contact Area ($mm^2$) | 25.00 |
| Gap, x (m) | 0.02 |
| Dielectric thickness, d (μm) | 100.00 |
| Surface charge density, σ ($\mu Cm^{-2}$) | 8.00 |

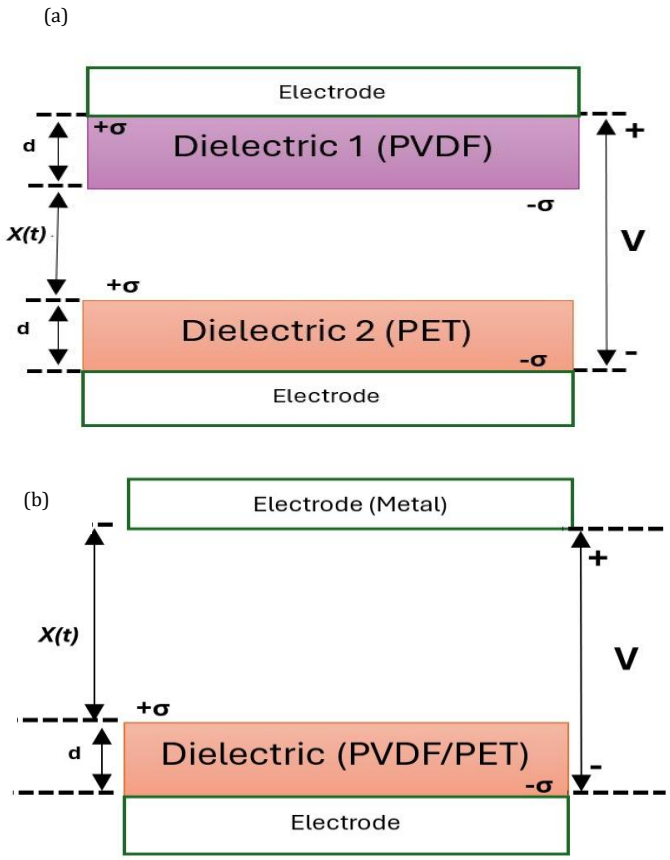


**Figure 1**. Schematic representation of the principles of TENGs based on PVDF/PET. Attached-electrode parallel plate contact mode TENGs are modeled schematically: (a) dielectric–dielectric and (b) metal–dielectric

model thus replicates the assembly, retraction, and subsequent triboelectric charging cycles in a frame-wide, sequence-resolved way, giving the simulation the necessary physical realism.

Furthermore, the analytic configuration incorporated the Faraday cage depicted in Figure 2, a critical requisite for ensuring the precision of the TENG's output assessment. The Faraday cage aided in eliminating external electromagnetic fields, which may obscure TENG's performance evaluation. Moreover, the entire measurement system, including the devices for measuring voltage, current, and charge density output of the TENG, was modeled in COMSOL Multiphysics. This was an important step as it prepared the model for parameterization, simulation, and data analysis, thus confirming the TENG model is accurate and fully represents the actual device.

In the last stage of the simulation procedure, the performance of the TENG's device was further optimized through an iterative process of changing key parameters and re-simulating and analyzing the resulting data. This iterative process involved adjusting the model's parameters, such as contact area, surface charge density, material properties, also repeating simulation and data analysis steps to identify optimal configurations for TENG devices.

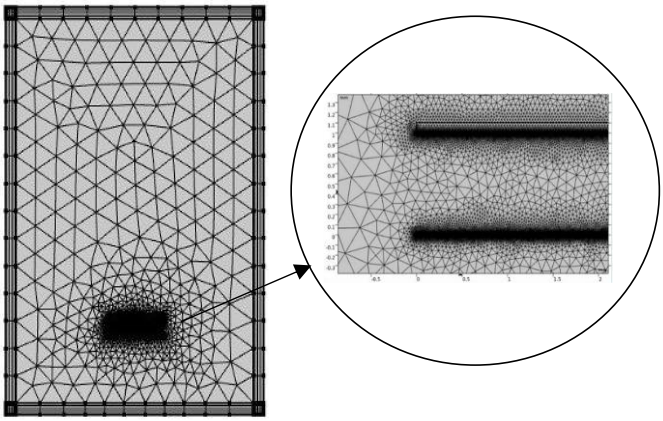

**Figure 2**. Simulation geometry of air boundary layer, enclosing two embedded media (PVDF/PET), which can model either a metal–dielectric stack or dielectric–dielectric arrangement

### 2.2. Simulation Metal–Dielectric

In the metal–dielectric principle, the dielectric having a larger work function than the metal will cause electrons to migrate from the metal surface to the dielectric. Specifically, open circuit output voltage ($V_{oc}$) and transferred charge in short circuit state ($Q_{sc}$), metal–dielectric simulation investigated the main output features of the device in contact separation mode.

For the purpose of theoretical comparisons, the relative permittivity, ε, of PET and PVDF was taken to be 3.7 and 7.5, respectively. A thickness of $d_1$ is 100 μm, interposed between electrodes of thickness $d_m$ is 1 μm, with dimensions of width, w is 5 mm, and length, *l* is 5 mm. The electrodes are distanced by 1 mm, and the tribo-charge surface density, σ is given as 8 μC/m$^2$. The system functions at a maximum separation distance of $x_{max}$ is 0.02 m and an average velocity of v is 1 m/s. The parameters that are varied during the simulation include contact area, surface charge density, gap, and dielectric thickness. The succeeding measurement records the simulation findings for voltage, current, and power density.

### 2.3. Simulation Dielectric–Dielectric

Generally, simulations of dielectric–dielectric devices offer a basis for comparison with metal–dielectric devices. Tribo-charges in the dielectric scenario led to the generation of free charges on the top electrode on both sides of the dielectric material, a phenomenon distinct from the surface charges present in metal–dielectric configurations. These tribo-charges are fixed on the material surfaces, creating opposite and equal charges, enforcing the conservation law for charge density to ensure the cancellation of all positive and negative charges. When contrasting metal–dielectric configurations with dielectric–dielectric setups, the main differences are found in the materials' work function, surface conditions, and material permittivity [6]. Table 2 presents the parameters of dielectric–dielectric PVDF/PET, showcasing the key properties and characteristics that define the performance of this material in various applications.

**Table 2.** Parameters of dielectric–dielectric PVDF/PET [10]

| Parameter | Value/Description |
|---|---|
| Contact Area ($cm^2$) | 6.45–58.06 |
| Gap (mm) | 2.54–25.40 |
| Dielectric thickness, d (μm) | 50.80–508.00 |
| Surface charge density ($pC/m^2$) | 328.50 |

## 2.4. Experimental

The high-sensitivity polymer piezoelectric film sensor was purchased from Amazon (Figure 3), comprising a PVDF film with screen-printed silver ink electrodes, adhered to a 0.125 mm PET substrate, and equipped with two crimped contacts. The Rockwell Hardness Testing Machine has been modified to operate as a mechanical press, exerting vertical compression on the sample via the indenter head [11]. The applied force used in the experiment ranges approximately between 1 and 10 N. To attach the testing items to a plate, conductive double-sided tape was used. A strip of tape was applied around the perimeter of each sample to verify the correct placement of the electrical connection.

A conductive tape strip will be attached as an electrode for evaluating each sample. Both surfaces will be manually grounded using a wire connected to the ground in between each randomized testing run. The samples will be placed on testing plates and secured with double-sided tape. To assist measurement, the tape electrodes will be secured with clips and connected to the multimeter. The experiment is illustrated in Figure 4.

## 3. DATA ANALYSIS AND RESULTS

### 3.1. Material Selection

PVDF helps to generate charge [7], and PET provides structural support and flexibility, while TENG design takes advantage of the fact that these two materials work well together [6]. The effective utilization of PVDF and its copolymers in self-powered devices, combined with the superior performance of PET as a positive tribo-material compared to PVDF, renders these materials a favorable selection for TENGs due to their synergistic performance and established reliability [6].

### 3.2. Results of Simulation Metal–Dielectric

Simulation findings of metal–dielectric reveal that the open-circuit voltage ($V_{oc}$) reached a peak of 311.3 V, along with a maximum power density of $2.9 \times 10^{-8}$ W. Furthermore, a maximum short-circuit transfer charge of 7.2366 C was observed, as outlined in Table 3. In photovoltaic and electronic devices, the open-circuit voltage represents the highest achievable voltage measurable when the device is disconnected from any external load. Consequently, the observed $V_{oc}$ stands at 311.3 V, indicating the device may reach this voltage without load. This parameter is significant since it has a direct impact on the highest power output achievable and the device's overall efficiency in the operational environment [12].

**Table 3.** Metal–dielectric simulation results

| Parameter | Simulation Result |
|---|---|
| Output Voltage (V) | 311.3 |
| Short circuit transfer charge (C) | 7.2366 |
| Power Density (W) | $2.9 \times 10^{-8}$ |

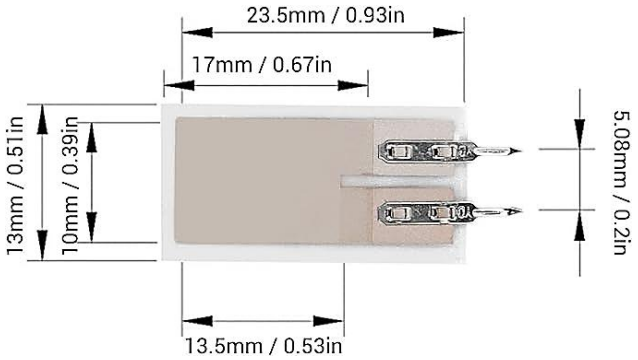


**Figure 3**. Dimensions of the PVDF/PET TENG device

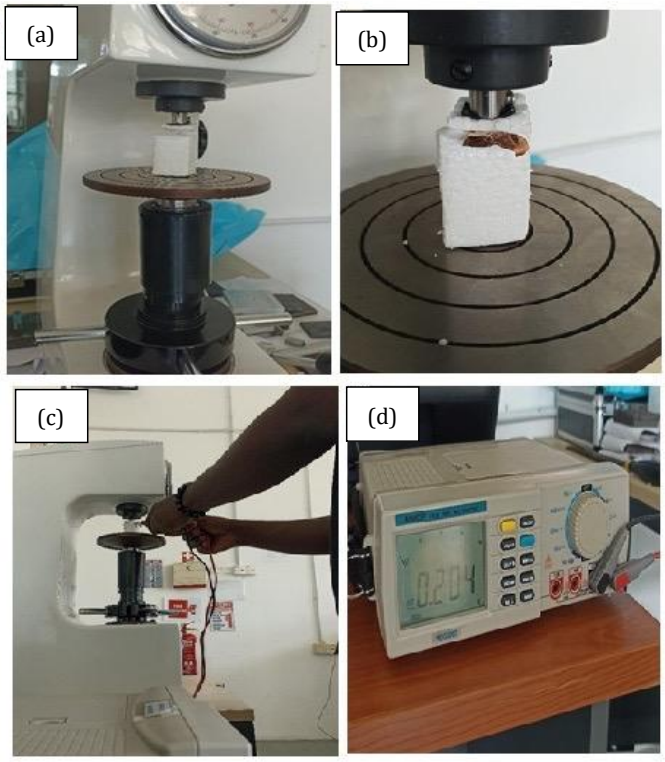


**Figure 4**. (a) Modified vertical linear stage for application of force. (b) Application of force to the device. (c) Measuring the output voltage. (d) Voltmeter showing the output voltage

The described power density maximum of $2.9 \times 10^{-8}$ W is the best power for the device to deliver on, a per-unit-area basis. This value is particular importance when considering devices that collect energy, such as nanogenerators or photovoltaic cells, as there is a need to maximize the power output to the size of the device. In TENGs, higher efficiency with respect to the device's mechanical to electrical energy conversion originates from the emphasis placed on surface charge density; more efficiency is attained via large power density improvements as a result of conversion [13]. The maximum quantity of charge that is transferred is limited to

7.2366 C. This indicates the total charge transfer when the output terminals of the device are connected. In the case of triboelectric nanogenerators, the area of contact and the degree of pressurization dictate the short-circuit current and hence the charge transferred. It has been claimed that the area of physical contact may limit the generated electrical power output, as the open circuit voltage and short circuit current appear to stabilize at higher levels of contact pressure. The observation offers information on the electric performance of the metal–dielectric system. Thus, understanding these factors is necessary for optimizing the device's design and material selection to fulfill goal criteria [14].

Figure 5(a) shows the energy potential for the PVDF/PET TENGs, illustrating potential changes across the dielectric when an external electric field is applied. Potential contours clearly mark areas of strong and weak fields. The sharp gradient appears close to the central electrode, indicating the composite reacts to the driving voltage. Insight is essential for tuning dielectric devices because the material's capacity to store and release charge directly affects overall performance.

As seen in Figure 5(b), the rate at which voltage increases with distance appears to be diminished, resembling a curve nearing a horizontal asymptote. This implies that above a certain point, voltage development becomes significantly constrained. This phenomenon is possibly due to signal strength, which is represented by voltage in this instance, increasing with distance until it stabilizes. The curve depicted in Figure 5(c) exhibits a non-linear increase that is decelerating in rate. In TENG models, charge or potential accumulates in various spatial configurations, especially since $\varepsilon_0$ and $\mu$ are commonly used in energy harvesting models. The graph also demonstrates that increasing distance yields progressively smaller results.

### 3.3. Results of Simulation Dielectric–Dielectric

According to the simulation results, the maximum output voltage recorded was 230 V, the maximum output current reached 1.5 mA, and the most elevated power density recorded was 3.2 W/m$^2$. These results imply that TENGs hold promise for generating significant power due to the higher dielectric thickness and surface charge density. This triboelectric nanogenerator produces acceptable power levels suitable for low-energy applications. These results, however, underline the need for careful tuning of design parameters, including dielectric thickness, surface charge density, electrode area, and output voltage, to achieve even higher current and power density [15].

As the dielectric gap size and effective contact area both increase, the power density also increases. For instance, altering the dielectric thickness from 50.8 µm to 508 µm raises the power density from 1.5 W/m$^2$ to 3.2 W/m$^2$, while elevating the output voltage from approximately 180 V to about 230 V, also increasing the surface charge density from 328.5 pC/m$^2$ to a peak of 2.3 nC/m$^2$. From this, it can be discovered that once the voltage rises, it practically doubles the power density. Table 4 collectively illustrates that as the dielectric thickness, surface charge density, gap distance, or contact area increases from their minimum to maximum values, both the output voltage and current increase.

**Table 4.** Dielectric–dielectric output simulation results

| Dielectric Thickness (µm) | Output Voltage (V) | Output Current (mA) | Power Density (W/m$^2$) |
|---|---|---|---|
| 50.8 | 180 | 1.20 | 2.5 |
| 152.4 | 200 | 1.30 | 2.8 |
| 254.0 | 215 | 1.40 | 3.0 |
| 355.6 | 225 | 1.45 | 3.2 |
| 508.0 | 230 | 1.50 | 3.2 |

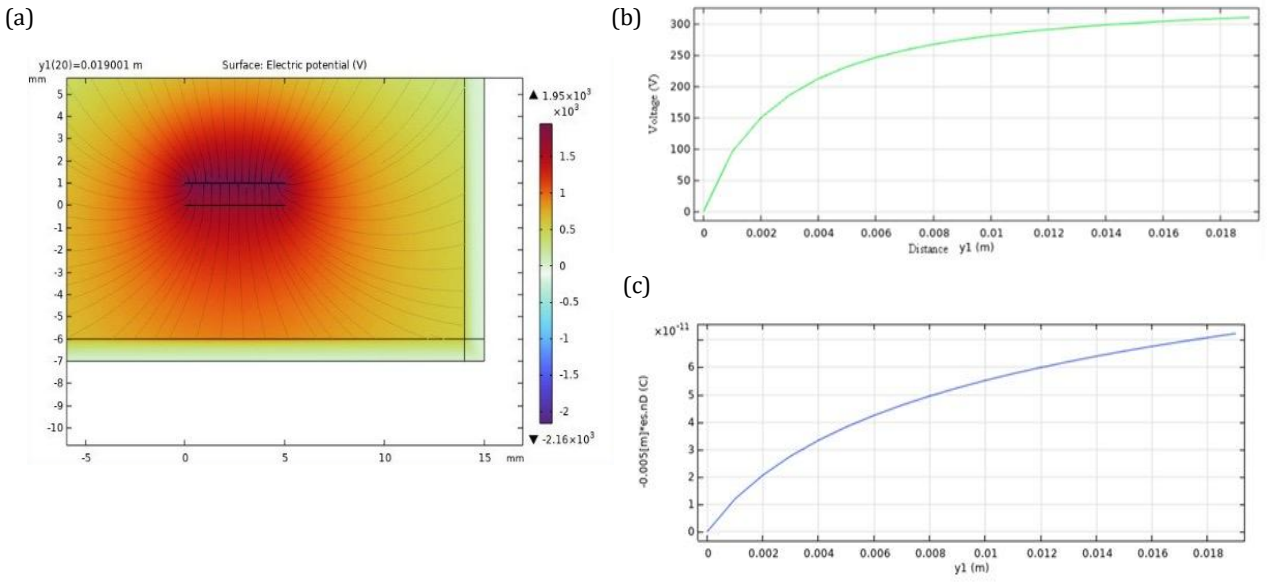


**Figure 5**. (a) Energy potential. (b) Graph of output voltage and distance. (c) Graph of surface and distance of metal–dielectric simulation result

The findings reported here have important consequences for refining triboelectric nanogenerators. Simulations indicate, as the dielectric layer thickness increases, the devices' performance enhances, raises the surface charge density, and expands both the mechanical gap and the area of contact during operation. Improvements like thicker insulation sheets or larger electrodes generate net advantages and practical potential for optimizing TENG production [16]. Figure 6 shows when the gap between the two surfaces widens, the system output-safety voltage, or stored charge, tends to rise, though the speed of that rise slowly tapers off. This behavior is frequent in electrostatic and energy-harvesting settings, where distance directly affects potential differences or the quantity of triboelectric charge that is swapped [16].

### 3.4. Results of Experimental

This experiment aims to analyze the relationship between the output voltage generated by PVDF-PET TENG and the different levels of mechanical force applied. The experimental TENG device, measuring 10 mm × 17 mm and 0.254 mm thick, was pressed with step loads of 1 N, 5 N, 7 N, and 10 N. After each load was held for a fixed interval, the resulting peak voltages were recorded and statistically evaluated.

The experimental data reveals a distinctly nonlinear relationship between applied force and the voltage produced, as shown in Figure 7. Although the output voltage rises steadily as additional force is applied, the rate of that increase diminishes with stronger loads. This trend aligns with the theory, greater force widens contact separation, liberating more triboelectric charge and yielding a higher potential difference. The curvature observed, however, indicates small contributions from material characteristics, surface roughness, and device geometry that modulate charge transfer in a manner not described by a simple linear model [17].

The properties of PVDF and PET are the most important factors affecting charge transfer efficiency of TENGs. Such a piezoelectric actuator is based on PVDF, in which the surface is subjected to force, an electric charge will be produced, and PET acts as the dielectric medium. When the insulating materials are separated from the work function, the difference induces electron transfer from PET to PVDF by contact electrification to generate a potential between electrodes. Increased deformation forces further increase the contact area and, hence, charge density but are subjected to the risk of recombination as a result of the lack of complete separation. Based on a previous study, this occurs because of the presence of fluorine atoms in PVDF, which provides efficient electron trapping that allows the capability of sustain AC output under cycling for several times [9].

In addition, surface roughness of PVDF/PET layers favors triboelectric charge generation. According to Jin *et al.* (2018), peeled-flat PVDF with PET or metal gives stabilized but limited TENG outputs, such as polarization-aligned dipoles and enlarged surface potential by three times. In the configurations, the material effects are isolated, and PVDF's tribonegativity can be demonstrated in the absence of topography doping [18].

The TENG device design dictates the contact area and gap control of PVDF and PET layers for an immediate scaling factor of triboelectric charge generation to larger areas under pressure. With higher force, the geometric confinement in fixed-dimensional setups stretches the real contact and opens the gaps between separation distances, leading to lower charge transfer and voltage saturation. The nonlinear voltage-force characteristic addresses cases of declining returns caused by capacitance changes and partial charge release [19].

The elevated output voltage recorded even under weak mechanical loads indicates that the PVDF/PET triboelectric

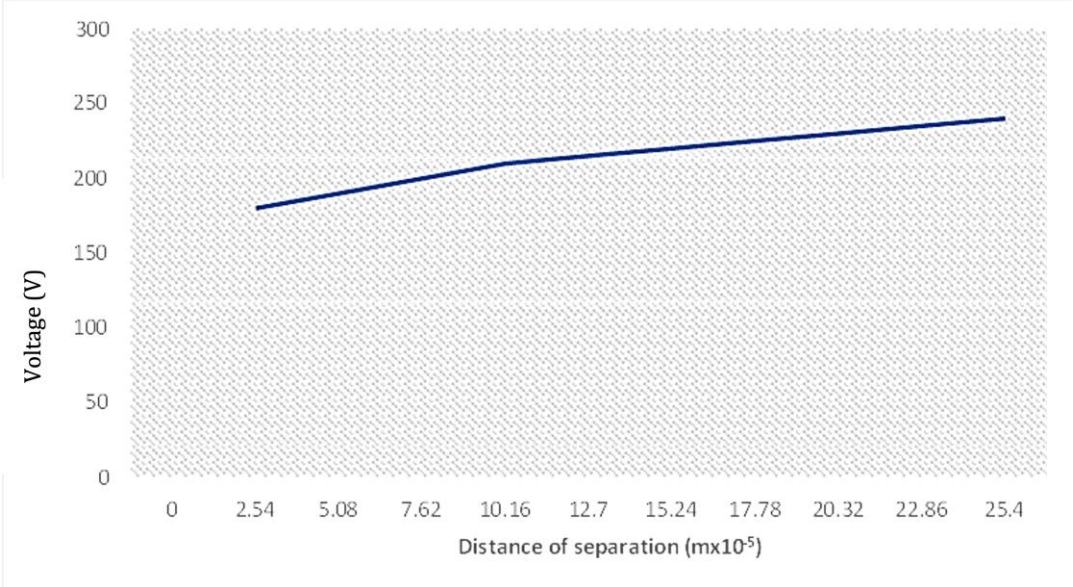


**Figure 6**. Graph of output voltage against the gap of the dielectric–dielectric

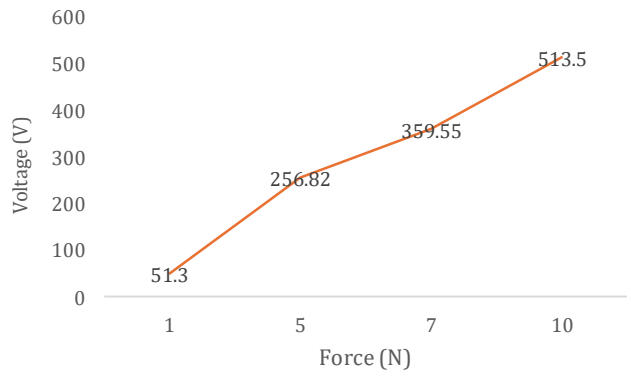


**Figure 7**. Dielectric–dielectric experimental results

nanogenerator converts mechanical work into electrical energy with outstanding efficiency, which is expected to be useful for specific applications. In real-world applications, the TENGs of wearable devices and sensors work well under the low-threshold forces (1–10 N) from walking or vibrations with enough power outputs (e.g., 3–40 V) that do not require high input force. Optimization for between 5–10 N thresholds, providing a consistent power output suitable for IoT devices, arthritis aids, and machinery vibrations, and optimum combination of charge density together with stability [20].

This TENG output voltage follows the classic model $V = Q/C$, where $Q = \sigma A$ relates to triboelectric charge density $\sigma$ influenced by work function difference $\Delta\phi$, and capacitance $C = (\epsilon_0 A)/d$ depends on permittivity ($\epsilon_0$), area ($A$), and separation ($d$). Force initially enlarges $A$ via deformation, boosting $Q$ and $V$, but beyond thresholds, increased $d$ and elasticity effects raise $C^{-1}$, causing nonlinear saturation as in PVDF-PET setups [21].

Also, this PVDF-PET TENG is expected to have long-term stability under cyclic low-intensity loads, for example, 5 to 10 N, from nonphysical activity or walking as well as vibration. This is due to the good mechanical resilience and fluorine-strengthened electron trapping of the β-phase PVDF, which endows the installed capacity against wear on the interface, which holds both charge density and contact area in reducing wear roughness [21]. These characteristics highlight their potential for dependable, durable energy harvesting in practical applications.

## 4. DISCUSSION

The results of the simulation indicate that the output voltage and current increase as the dielectric thickness and surface charge density increase. This is attributed to the larger surface charge area, dielectric thickness value, and the potential voltage difference between the two electrodes, which voltage is applied, resulting in elevated output charges and currents, as demonstrated [22]. Furthermore, power density was positively correlated with both increasing gap dimension and expanding contact area. This trend shows that, within the fixed electrode architecture used, the triboelectric nanogenerators attain heightened power production when electrode surfaces move closer together and the effective area of contact is maximized [17].

The simulation outcomes corroborate earlier studies of energy harvesting via TENGs, particularly with respect to quantitative performance indicators. Vasandani *et al.* (2016), for example, used a design-of-experiment framework with quantitative voltage measurements to systematically study the dependency of output voltage on structural design parameters. The analysis revealed a linear attenuation of output voltage as a function of increasing triboelectric layer thickness, whereas modulation of the dielectric spacers' separation distance produced a parabolic response, both of which are implicated in the electrostatic field's effective collapse on energy extraction efficiency [10].

The results demonstrate that the relationship between the externally applied pressure and the following electrical voltage generation exhibits a significant nonlinearity. Concerning the relationship between force and voltage, the resulting voltage demonstrates a distinct and steady trend in which it rises with an increase in the applied force. According to theory, an increase in force is expected to enhance the separation of contact, thus increasing the generation of triboelectric charge and the resultant voltage. Nonetheless, the relationship seems to be nonlinear, indicating that additional factors like the device's structural parameters and the materials employed in construction may influence the produced voltage [23].

The TENG devices exhibit significant high voltages even at low force levels. From a practical standpoint, this suggests that PVDF/PET TENGs have a high efficacy in converting mechanical work or mass energy into electrical energy. This extraordinary feature makes it a good alternative in energy harvesting systems, where slight mechanical activities can be transformed into electrical energy. In terms of nonlinearity and device optimization, the non-linear relationship between voltage and force suggests that further optimization can be achievable. It is feasible to enhance the thickness ratio between PVDF and PET, address surface irregularities, and optimize the electrode configuration. Moreover, determining the saturation point beyond which additional pressure does not notably increase the output voltage is valuable for practical applications.

## 5. CONCLUSIONS

It is shown in this study that increasing the dielectric separation or thickness in dielectric–dielectric TENGs always leads to a positive contribution to both the output voltage and power density, which certifies that the voltage was the dominant parameter in determining the performance. The excellent correspondence between simulation and experimental voltage–distance trends corroborates the proposed electrostatic or triboelectric models, which demonstrate that there is saturation at large gaps due to charge equilibrium and field redistribution, defining an optimal dielectric thickness that could result in efficient energy conversion. Additionally, the PVDF/PET material strategy is demonstrated to be an efficient combination of materials, the micromorphology of which displays a perfect match and provides combination

prototype with stronger open-circuit voltage and current density performance in both simulated and practical manners. Theoretical prediction and experimental measurement demonstrate that additional betterment of contact pressure, electrode geometry, and operating dynamics can boost not only the power density but also stable output in response to low-force intermittent excitation, offering explicit design advances for miniaturized self-powered sensors and energy harvesters.

**REFERENCES**


[1] J. L. Holechek, H. M. E. Geli, M. N. Sawalhah, and R. Valdez, "A Global Assessment: Can Renewable Energy Replace Fossil Fuels by 2050?," *Sustainability*, vol. 14, no. 8, p. 4792, 2022.

[2] A. E. Akin-Ponnle and N. B. Carvalho, "Energy Harvesting Mechanisms in a Smart City—A Review," *Smart Cities*, vol. 4, no. 2, pp. 476–498, 2021.

[3] X. Álvarez, E. Valero, N. de la Torre-Rodríguez, and C. Acuña-Alonso, "Influence of Small Hydroelectric Power Stations on River Water Quality," *Water*, vol. 12, no. 2, p. 312, 2020.

[4] K. Obaideen *et al.*, "Solar Energy: Applications, Trends Analysis, Bibliometric Analysis and Research Contribution to Sustainable Development Goals (SDGs)," *Sustainability*, vol. 15, no. 2, p. 1418, 2023.

[5] H. Zhang, L. Yao, L. Quan, and X. Zheng, "Theories for triboelectric nanogenerators: A comprehensive review," *Nanotechnology Reviews*, vol. 9, no. 1, pp. 610–625, 2020.

[6] Z. Zhao, Y. Lu, Y. Mi, J. Meng, X. Cao, and N. Wang, "Structural Flexibility in Triboelectric Nanogenerators: A Review on the Adaptive Design for Self-Powered Systems," *Micromachines*, vol. 13, no. 10, p. 1586, 2022.

[7] L. Shi *et al.*, "High-performance triboelectric nanogenerator based on electrospun PVDF-graphene nanosheet composite nanofibers for energy harvesting," *Nano Energy*, vol. 80, p. 105599, 2021.

[8] L. Cheng, Q. Xu, Y. Zheng, X. Jia, and Y. Qin, "A self-improving triboelectric nanogenerator with improved charge density and increased charge accumulation speed," *Nature Communications*, vol. 9, no. 1, p. 3773, 2018.

[9] C. Li *et al.*, "High-Performance Triboelectric Nanogenerator Based on PVDF Nanofibers Modified by a Charge Control Agent n-Propyl Gallate," *Materials*, vol. 18, no. 13, p. 3089, 2025.

[10] P. Vasandani, Z.-H. Mao, W. Jia, and M. Sun, "Design of simulation experiments to predict triboelectric generator output using structural parameters," *Simulation Modelling Practice and Theory*, vol. 68, pp. 95–107, 2016.

[11] S. S. Murugan, "Mechanical Properties of Materials: Definition, Testing and Application," *International Journal of Modern Studies in Mechanical Engineering*, vol. 6, no. 2, pp. 28–38, 2020.

[12] D. R. Ahmed and F. F. Muhammadsharif, "A Review of Machine Learning in Organic Solar Cells," *Processes*, vol. 13, no. 2, p. 393, 2025.

[13] Y. Qin and Q. Xu, "Enhancing Surface Charge Density of Materials," in *Handbook of Triboelectric Nanogenerators*, Cham: Springer International Publishing, 2023, pp. 1411–1436.

[14] H. Zou, "Quantification of Triboelectric Charge Density for a Solid," in *Handbook of Triboelectric Nanogenerators*, Cham: Springer International Publishing, 2023, pp. 243–291.

[15] X. Kang, C. Pan, Y. Chen, and X. Pu, "Boosting performances of triboelectric nanogenerators by optimizing dielectric properties and thickness of electrification layer," *RSC Advances*, vol. 10, no. 30, pp. 17752–17759, 2020.

[16] M. Wajahat, A. Z. Kouzani, S. Y. Khoo, and M. A. P. Mahmud, "Comparative study and multi-parameter analysis to optimize device structure of triboelectric nanogenerators," *Nanotechnology*, vol. 34, no. 42, p. 425403, 2023.

[17] Z. L. Wang, "From contact electrification to triboelectric nanogenerators," *Reports on Progress in Physics*, vol. 84, no. 9, p. 096502, 2021.

[18] J. P. Lee, J. W. Lee, and J. M. Baik, "The Progress of PVDF as a Functional Material for Triboelectric Nanogenerators and Self-Powered Sensors", *micromachines*, vol.9, no. 10, p. 532, 2018.

[19] J. Jeong, J. Ko, and J. Lee, "Dual polarity open circuit voltage in triboelectric nanogenerators originated from two states series impedance," *Discover Nano*, vol. 19, p. 111, 2024.

[20] K. R. S. D. Gunawardhana, N. D. Wanasekara, and R. D. I. G. Dharmasena, "Towards Truly Wearable Systems: Optimizing and Scaling Up Wearable Triboelectric Nanogenerators," *iScience*, vol. 23, no. 8, p. 101360, 2020.

[21] I. Aazem et al., "Electroactive phase dependent triboelectric nanogenerator performance of PVDF–$TiO_2$ composites", *Energy Advances*. vol. 4, no. 5, pp.683-698, 2025.

[22] S. Fu *et al.*, "Conversion of Dielectric Surface Effect into Volume Effect for High Output Energy," *Advanced Materials*, vol. 35, no. 40, p. 2302954, 2023.

[23] J. Wang, S. Xu, and C. Hu, "Charge Generation and Enhancement of Key Components of Triboelectric Nanogenerators: A Review," *Advanced Materials*, vol. 36, no. 50, p. 2409833, 2024.